EPIDEMIOLOGY

Predicting pathogen mutual invasibility and co-circulation

Sang Woo Park[1,2]*, Sarah Cobey[2], C. Jessica E. Metcalf[1], Jonathan M. Levine[1], Bryan T. Grenfell[1]*

Observations of pathogen community structure provide evidence for both the coexistence and replacement of related strains. Despite many studies of specific host-pathogen systems, a unifying framework for predicting the outcomes of interactions among pathogens has remained elusive. We address this gap by developing a pathogen invasion theory (PIT) based on modern ecological coexistence theory and testing the resulting framework against empirical systems. Across major human pathogens, PIT predicts near-universal mutual susceptibility of one strain to invasion by another strain. However, predicting co-circulation from mutual invasion also depends on the degree to which susceptible abundance is reduced below the invasion threshold by overcompensatory epidemic dynamics, and the time it takes for susceptibles to replenish. The transmission advantage of an invading strain and the strength and duration of immunity are key determinants of susceptible dynamics. PIT unifies existing ideas about pathogen co-circulation, offering a quantitative framework for predicting the emergence of novel pathogen strains.

Understanding the factors that allow the coexistence or exclusion of pathogen variants is a fundamental challenge in the dynamics and control of infectious diseases (*1*–*4*). Progress requires better understanding of how competition occurs by means of the host immune response and its implications for the invasion of new strains. Despite many studies of specific host-pathogen interactions (*5*–*10*), no unifying framework exists to explain invasion dynamics and subsequent competitive outcomes across pathogen systems. The continued emergence of novel pathogens and ongoing vaccine development against antigenically variable threats emphasize the importance of this question (*11*).

A major challenge in developing a unifying framework for pathogen community structure is explaining the heterogeneity of observed competitive outcomes across pathogens. Specifically, understanding what mechanisms promote stable coexistence among some pathogen variants (Fig. 1, A to C) but not others (Fig. 1, D to E). For example, notwithstanding heterogeneity in the observed dynamics, stable coexistence in large host populations is maintained between respiratory syncytial viruses (RSV) A and B (Fig. 1A), Coxsackievirus A16, Enterovirus A71 (Fig. 1B), and four dengue serotypes (Fig. 1C). On the other hand, the evolutionary dynamics of severe acute respiratory syndrome coronavirus 2 (SARS-CoV-2) variants (Fig. 1D) and seasonal influenza strains of the same subtype (Fig. 1E) exemplify strain replacement patterns, in which the emergence of antigenically distinct variants causes extinction of previously dominant variants (*5*, *7*, *12*).

To explain these heterogeneous outcomes, we present a unifying framework for predicting whether a pathogen variant can invade a host population in the presence of their competitor. We show that predicting co-circulation from invasion depends on changes in the susceptible pool following invasion. Specifically, the invading pathogen will continue to infect susceptible hosts even as a given epidemic declines past its peak, driving the susceptible pool below the invasion threshold. Therefore, the pathogen overcompensates by using up more susceptible resources than it requires and can prevent itself and its competitor from reinvading until the susceptible pool is replenished. We quantify this overcompensation using two measures: maximum reduction in the susceptible pool, and the time it takes for the susceptible pool to replenish to permit reinvasion. In doing so, we explore how the transmission advantage of the invading variant and underlying immune structures affect this overcompensatory dynamics.

[1]Department of Ecology and Evolutionary Biology, Princeton University, Princeton, NJ 08540, USA. [2]Department of Ecology and Evolution, University of Chicago, Chicago, IL 60637, USA.
*Corresponding author. Email: swp2@princeton.edu (S.W.P.); grenfell@princeton.edu (B.T.G.)

Pathogen invasion theory

Many models have been proposed to explain observed patterns of competition for specific pathogen systems (*1*, *11*, *12*, *13*–*19*) and to identify the mechanisms that dictate persistence and coexistence following the invasion of new variants (*7*, *20*). However, these models rely on detailed assumptions, often specific to the pathogen, making it difficult to draw general conclusions about pathogen competition across different systems. So far, there is no single overarching framework that allows quantitative comparisons of coexistence potential across different pathogen systems.

To unify heterogeneous patterns of pathogen competition, we have developed the pathogen invasion theory (PIT), inspired by Chesson's modern coexistence theory (MCT) from community ecology [see the supplementary materials (SM) section S1] (*21*). Specifically, PIT allows us to simplify any system of two competing pathogen variants i and j into two quantities that determine their invasibility (SM sections S2 and S3). First, the immunological niche difference 1−ρ describes the ability of a variant to escape the host's immune response induced by another variant. This is measured as a ratio of equilibrium values (or long-term averages) of geometric mean of intraspecific susceptibility ($\sqrt{S_{i|i}S_{j|j}}$) versus interspecific susceptibility ($\sqrt{S_{j|i}S_{i|j}}$) at the population level:

$$1-\rho = 1-\sqrt{\frac{S_{i|i}S_{j|j}}{S_{j|i}S_{i|j}}}, \quad (1)$$

where $S_{j|i}$ represents the effective proportion of individuals who are susceptible to variant j. when variant i is at equilibrium; note that equilibrium conditions arise when the amount of susceptible individuals is balanced with the basic reproduction number: $\mathcal{R}_{0,i}S_{i|i=1}$. Second, the fitness difference, f_i / f_j, measures the ratio of each variant's innate ability to spread ($\mathcal{R}_{0,i}$ and $\mathcal{R}_{0,j}$), discounted by its susceptibility to the host immune response to the other variant:

$$\frac{f_i}{f_j} = \sqrt{\frac{\mathcal{R}_{0,i}S_{i|j}}{\mathcal{R}_{0,j}S_{j|i}}} \quad (2)$$

Then, similar to MCT (*21*), the immunological niche difference bounds the fitness differences compatible with mutual invasion, the condition under which two competing species (in this case, pathogen variants) can invade one another when the other species is at equilibrium. In short, the greater niche difference 1−ρ (likewise, the smaller niche overlap ρ), the more easily competitively imbalanced strains can mutually invade, satisfying the following inequality:

$$\rho < \frac{f_i}{f_j} < \frac{1}{\rho}. \quad (3)$$

Importantly, all quantities necessary to inform the immunological niche difference and the fitness difference ($\mathcal{R}_{0,i}, S_{i|j}$) can be derived from epidemiological models tailored to individual diseases, allowing for quantitative comparisons across systems.

Mutual invasion is often associated with long-term, stable coexistence in the classical MCT (*21*) and in the broader ecological and evolutionary literature (*22*, *23*). However, nonlinear host-pathogen interactions, especially immunological feedbacks, add challenges to translating mutual invasibility to predictions about prolonged pathogen co-circulation, a key requirement for maintaining diversity of pathogen strains (*24*). Here, we begin by comparing invasibility across pathogen systems and then turn to predicting pathogen co-circulation from invasibility.

Comparative pathogen invasion dynamics

We quantify mutual invasibility of various pathogen variant pairs by applying PIT (SM

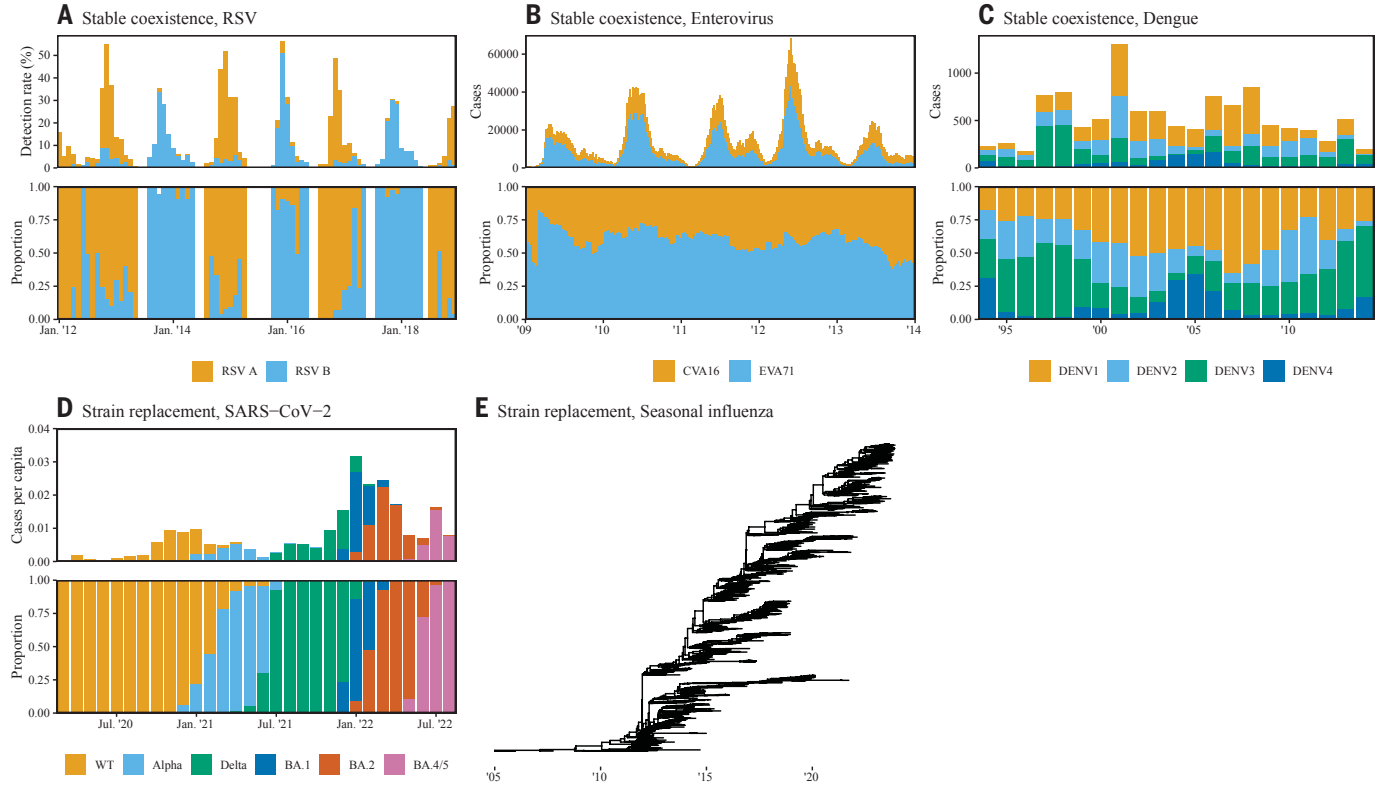

Fig. 1. Observed coexistence patterns of human pathogens. (**A**) Monthly detection rates of RSV A and B (top) and their relative proportions (bottom) from Cheonan, Korea (*41*). (**B**) Weekly cases of hand, foot, and mouth disease caused by CV-A16 and EV-A71 (top) and their relative proportions (bottom) from all 31 provinces of mainland China (*42*). (**C**) Annual cases of four dengue serotypes (top) and their relative proportions (bottom) from Bangkok, Thailand (*43*). (**D**) Monthly per capita cases of SARS-CoV-2 variants (top) and their relative proportions (bottom) from 10 representative countries (*12*). (**E**) Phylogenetic tree of 1578 human influenza A H3N2 subtype genome sampled between 2005 and 2023, publicly available on https://nextstrain.org/. All data are taken from publicly available sources from the above references.

section S4) to a diverse set of empirically motivated models of multistrain pathogen dynamics (*1*, *11*–*19*). The results are plotted in Fig. 2, in which the region of mutual invasibility is bounded by Eq. 3. The boundaries of mutual invasibility, predicted by PIT, are equivalent to those predicted for ecological communities by MCT (*21*).

For nearly all pathogen variant pairs tested, PIT predicts mutual invasion (Fig. 2). Two main factors contribute to this near universality of mutual invasibility: First, infection with one variant almost always confers weaker heterotypic (cross) immunity against other related pathogens, or their respective variants, than homotypic immunity, creating distinct immunological niches. Second, many closely related pathogens or pathogen variants have similar $\mathcal{R}_0$, which causes limited variation in the resulting fitness difference; when $\mathcal{R}_0$ is similar, even a small advantage in cross immunity ($S_{i|i} < S_{j|i}$, $S_{j|j} < S_{i|j}$) can be sufficient to allow for mutual invasion. For example, these two factors that favor mutual invasion apply to antigenically variable strains of seasonal influenza, for which strain replacement is the norm (*5*, *25*–*27*).

However, not all pathogen variants have similar $\mathcal{R}_0$, in which case larger immunological niche differences are required for mutual invasion. For example, pathogens in the Paramyxovirus family exhibit 15 to 70% difference in $\mathcal{R}_0$ (*10*) but still permit mutual invasion. Another key example is provided by SARS-CoV-2 variants, for which we predict mutual invasion despite large differences in $\mathcal{R}_0$ driving strain replacement patterns (*28*, *29*). Accounting for the effects of vaccination (fig. S1), or assuming a greater transmission advantage (fig. S2), prevented the SARS-CoV-2 wild-type variant from invading the SARS-CoV-2 Alpha variant; however, mutual invasibility predictions for all other variants are generally robust across different assumptions about vaccination, increased transmissibility, and cross immunity (SM section S8; figs. S1 to S3).

One exception to mutual invasibility is smallpox in competition with mpox; in this case, PIT predicts that the endemic presence of smallpox would prevent the invasion of mpox. This prediction is consistent with previous hypotheses that mpox invasion was only possible because of smallpox eradication and the eventual waning of immunity against smallpox (*2*, *18*).

The apparent contradiction between the predicted mutual invasibility of seasonal influenza strains and SARS-CoV-2 variants (Fig. 2) and the observed patterns of competitive replacement (Fig. 1) raises a critical question of what mechanisms determine the co-circulation versus replacement of variants that can mutually invade one another.

Mutual invasion, persistence, and co-circulation

Given mutual invasion, the fate of pathogen competition following invasion is determined by the extent of overcompensatory susceptible depletion dynamics, which can prevent both competitors from reinvading the host population (*5*, *6*). When overcompensation is strong, co-circulation requires both resident and invading variants to effectively persist until the susceptible pool is replenished. Although overcompensatory effects can be also found in other ecological systems, including predator-prey systems, most MCT analyses and interpretation of the mutual invasion condition either (*1*) focus on systems that experience limited overcompensation and do not exhibit large population cycles or (*2*) allow for long

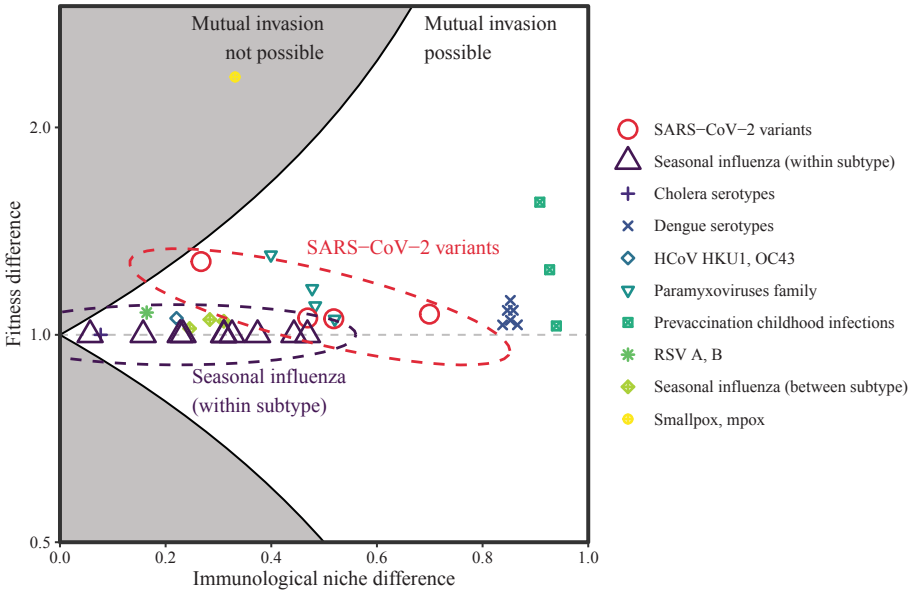

Fig. 2. Quantifying coexistence patterns of different human pathogen variant pairs. Niche and fitness difference estimates across different human pathogen variants in the absence of vaccination. Each point indicates a pairwise comparison of pathogen variants from various systems, indicated by the associated shape. Comparisons for prevaccination childhood infections consider ecological interference between measles versus chickenpox, rubella, and whooping cough (*1*). Points in the white region allow mutual invasion, meaning that a variant can invade a population when the competing variant is at equilibrium. The yellow point (smallpox and mpox) within the gray region does not allow mutual invasion, meaning that the presence of a more fit variant (smallpox) prevents the invasion of a less fit variant (mpox). Dashed ellipses indicate SARS-CoV-2 variant pairs and within-subtype seasonal influenza strain pairs, which exhibit strain replacement patterns. We plot max (f_i/f_j, f_j/f_i) such that the fitness difference is always greater than 1. The fitness difference is plotted on a log scale for symmetry.

time scales for recovery from vanishingly low densities (*21*, *30*). For overcompensating pathogen systems without persistent reservoirs, such recovery over long time scales is infeasible as a result of demographic stochasticity.

To illustrate how overcompensatory dynamics shape the outcome of pathogen interactions, we begin with a classic RSV model, which predicts that the invasion of either RSV A or B will cause both competitors to quickly settle into their respective endemic cycles (Fig. 3A). Specifically, these cycles match observed dynamics from outbreaks in Finland (*15*). This contrasts with the strain replacement pattern observed with SARS-CoV-2 variants and within influenza subtypes (Fig. 1, D and E). What factors allow RSV, but not SARS-CoV-2 or influenza, to overcome these overcompensatory effects?

To synthesize the different competitive outcomes across these three major pathogen systems, we explore how changes in the duration of immunity and transmission advantage of the invading variant affect the competitive outcome (Fig. 3D). In doing so, we summarize changes in the susceptible pool using two key measures: the degree of overcompensation (Fig. 3E) and the return time (Fig. 3F). The degree of overcompensation—defined as the maximum reduction in the effective reproduction number $\mathcal{R}(t)$ [i.e., 1 − min ($\mathcal{R}(t)$)]—captures the extent to which the susceptible pool is reduced below an invasion threshold. The return time—defined as the time until $\mathcal{R}(t)$ is increased above 1 for the first time after invasion—measures the amount of time it takes for the susceptible pool to replenish to permit reinvasion. As we illustrate below, the degree of overcompensation is mostly related to the transmission advantage of the invading variant, whereas the return time is affected by both. Using $\mathcal{R}(t)$ allows us to measure changes in the susceptible pool relative to $\mathcal{R}_0$. We specifically focus on measuring the degree of overcompensation and return time using $\mathcal{R}(t)$ of the resident variant to characterize its ability to persist following the invasion of a competing variant. Previous studies have explored how immunological details affect the co-circulation of pathogens (*5*, *20*), but susceptible dynamics often exhibit complex cycles, making them difficult to interpret. Summarizing the susceptible dynamics into the degree of overcompensation and return time both simplifies and reveals how changes in the duration of immunity and transmission advantage of the invading variant translate to changes in susceptible depletion dynamics, which in turn determine the competitive outcome.

We first identify conditions that allow co-circulation of mutually invading pathogens. Short-term immunity and limited transmission advantage (e.g., RSV) cause limited overcompensation (Fig. 3E) and fast return time from the overcompensated state (Fig. 3F), resulting in prolonged co-circulation without local extinction of either variant (Fig. 3D, yellow region). Pneumococcal serotypes, in which the underlying dynamics exhibit limited overcompensation, also experience this regime (*8*). In the case of limited overcompensation, PIT allows us to quantify how different immune mechanisms contribute to the maintenance of diversity (SM sections S6 and S9; fig. S4). In what follows, we show that the replacement of mutually invading strains can be caused by either severe overcompensation or modest overcompensation coupled with a slow return time.

Under a large transmission advantage, the invasion of a more transmissible variant can result in strong overcompensation (Fig. 3E) and slower return times to a state that permits further invasion (Fig. 3F) even when the duration of immunity of the invading variant is short. This effect can prevent the less transmissible variant from reinvading until the susceptible pool is replenished and causes strain replacement despite mutual invasion (Fig. 3D, green region). This prediction suggests that the increased transmissibility of successive SARS-CoV-2 variants (*28*, *29*, *31*) likely allowed for strong overcompensation, thereby preventing past variants from reinvading the population (Fig. 3B). This prediction is further supported by invasion simulations from a realistic SARS-CoV-2 model, which shows that increased transmissibility is required to drive past variants extinct (SM section S10; figs. S5 to S7).

Finally, longer-term immunity can lead to a slow return time (Fig. 3F), which for example explains the replacement among seasonal influenza strains within a subtype (Fig. 3, C and D). In fact, when the duration of immunity is very long, replenishment of the susceptible pool has to rely primarily on the birth of susceptible hosts, which can be very slow. This can prevent both resident and invading strains from reinvading the population after an outbreak, causing the eventual extinction of both strains. We note that whether the invading strains can persist or experience eventual extinction is likely indistinguishable in practice when new strains keep emerging as a result of antigenic drift or shift. These observations are further supported by more detailed influenza simulations, which show that prolonged immunity against individual seasonal influenza strains of the same subtype (*32*, *33*) makes co-circulation rare despite near-universal mutual invasibility (SM sections S7 and S11; figs. S8 to S10).

This conclusion is robust to assumptions about the strength of cross immunity, with

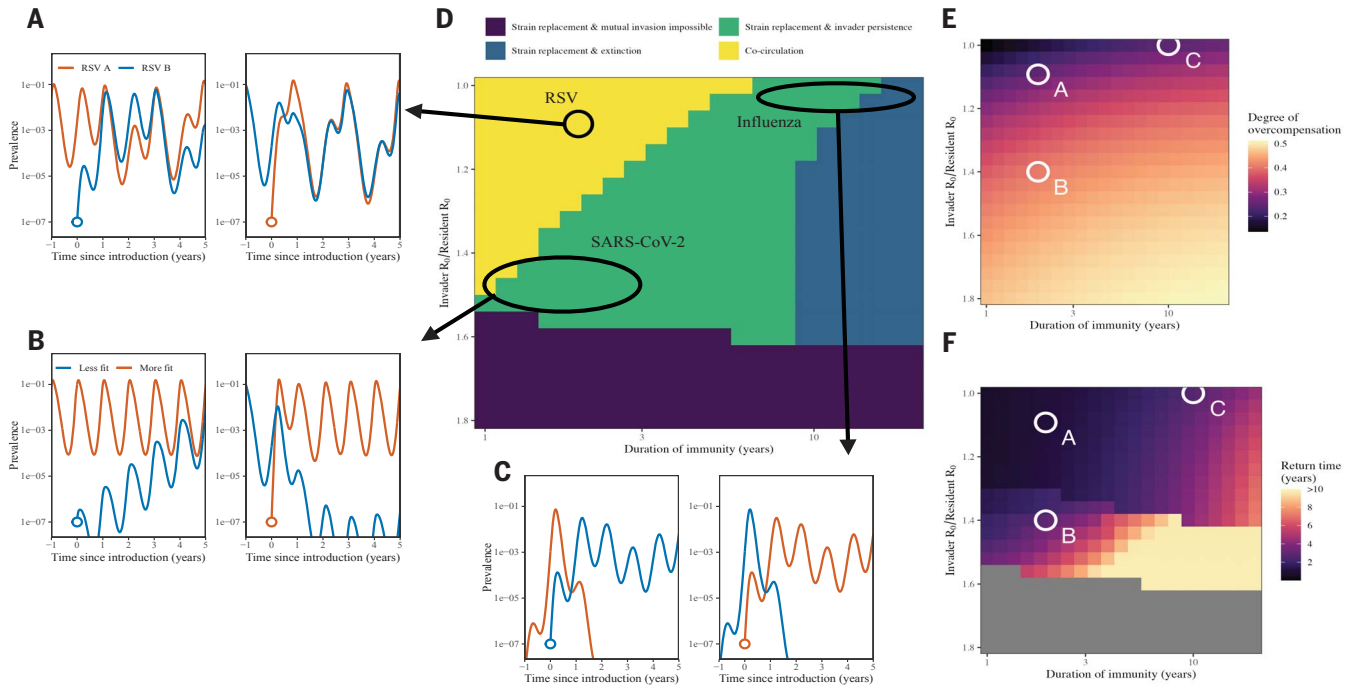

Fig. 3. Effects of epidemiological and immunological factors on overcompensatory dynamics and competitive outcomes. (**A**) to (**C**) Example mutual invasion simulations that capture competitive outcomes of (A) RSV subtypes, (B) SARS-CoV-2 variants, and (C) seasonal influenza strains within each subtype. Simulations assume (A) parameter estimates from (*15*); (B) 40% higher R0 for the more fit variant (orange); and (C) equal R0 for both variants and 10 years for the average duration of immunity, which is defined as the average time that a recovered individual returns to a fully susceptible state. All other parameters are from (*15*), including immune escape values which assume stronger homotypic immunity (64% protection) than heterotypic immunity (16% protection). (**D**) Competitive outcomes based on 10 years of simulations following the invasion of a novel variant while the resident is at equilibrium. Mutual invasion is possible in yellow, green, and blue regions. Mutual invasion is not possible in the purple region. 10-year persistence of both resident and invading variants is used as a minimum threshold for long-term co-circulation. Persistence and extinction is distinguished by a prevalence cutoff of 10^{-7}. All other parameters were fixed to previously estimated values. (**E** and **F**) Estimates of the degree of overcompensation and return time for the resident variant, corresponding to simulations in (D). For illustrative purposes, seasonal transmission was not included for simulations in (D) to (F). The standard RSV model by (*15*) was used for all simulations.

weaker cross immunity creating a larger immunological niche difference, leading to wider regions of mutual invasibility (fig. S11). Furthermore, faster return time results in wider regions of co-circulation.

Summary

There has been extensive work analyzing the invasion and coexistence of pathogen variants across many individual host-pathogen systems; however, synthesis and comparison across systems have been limited. We present a unifying framework, PIT, that allows for such comparison by quantifying key coexistence metrics—niche and fitness differences—in two-pathogen systems through the analysis of mechanistic models (fig. S13). PIT reveals that mutual invasion of initially rare variants is nearly universal for major pathogen systems, including exemplary systems of strain replacement such as seasonal influenza and SARS-CoV-2. Mutual invasibility implies stable coexistence among pairs of competitors in standard ecological systems (*21*).

By contrast, mutual invasibility hardly guarantees co-circulation in the pathogen systems we analyzed. Instead, the outcome of pathogen competition depends on the extent to which susceptible hosts are reduced below the invasion threshold (i.e., the degree of overcompensation) and the amount of time it takes for the susceptible pool to replenish (i.e., the return time) (*6*). Specifically, a greater transmission advantage of an invading variant and more durable immune protection can cause stronger overcompensation and slower return time, which can lead to variant replacement. Comparisons of coexistence dynamics of RSV subtypes, SARS-CoV-2 variants, and seasonal influenza strains demonstrate the importance of understanding the overcompensatory nature of susceptible depletion in predicting outcomes of pathogen competition.

Caveats and future directions

A key limitation of PIT is that it relies on pairwise comparisons. This contrasts with observed competition patterns (Fig. 1), which may depend on multistrain interactions (e.g., dengue serotypes) as well as the evolutionary history of antigenically variable strains (e.g., seasonal influenza and SARS-CoV-2). Therefore, predicting coexistence and replacement for pathogens that exhibit these characteristics would require detailed epidemiological models. In fact, extending pairwise predictions about coexistence to predictions about coexistence of multiple species is a major challenge in community ecology, particularly because of the presence of higher-order interactions (*34*). Predicting the effects of multipathogen interactions and evolutionary history on pathogen invasion and coexistence is an important area for future work (*7*).

Our PIT analysis centers around major, endemic pathogen systems, leaving the applicability of our findings to other pathogen systems as a topic for future work. Nonetheless, we generally expect conclusions about the near-universality of mutual invasibility to be robust given that they hold for exemplary systems of replacement (i.e., seasonal influenza and SARS-CoV-2). While PIT relies on predicting invasion into a resident system at equilibrium (and analogously, during stable epidemic cycles), the dynamics of many pathogens, especially those that exhibit strain replacement patterns, can be far from the equilibrium. Understanding

how invasibility changes across time, specifically in relation to the timing of past speciation of major pathogen lineages, will be crucial for predicting the future emergence of new pathogens. Comparing the impact of alternate formulations on niche and fitness differences as well as predictions of the final outcome of the competition will be also an important area for future work.

We focus on transmission advantage and duration of immunity as key variables that determine co-circulation. However, there are many other factors that maintain the diversity of pathogens, including evolutionary constraints (*35*) and other immunological mechanisms, such as strains that transcend immunity (*5*). Although our analysis does not account for these factors, our framework allows us to test whether new pathogens arising under these constraints can mutually invade, providing a tool to directly quantify the effects of various epidemiological and immunological factors on co-circulation.

Our invasion analysis focuses on competition within single, well-mixed host populations and therefore neglects spatial variation. This likely renders our predictions about pathogen coexistence conservative. In reality, heterogeneity in population dynamics across space can play an important role in determining overcompensation and maintaining pathogen persistence (*36*). Seasonality can also affect overcompensation and contribute to pathogen persistence (*37*). Despite these limitations, our work provides a quantitative foundation for understanding pathogen co-circulation.

Conclusion

The recent emergence and reemergence of novel pathogens has caused considerable societal disruption, emphasizing the need for better surveillance and control strategies to prevent future outbreaks. The near universality of pathogen mutual invasibility raises a serious public health concern given the potential recombination among variants and the emergence of new pandemic variants (*38*). Our results further underline the importance of global pathogen and immunological surveillance platforms for clarifying the dynamics of a potentially diverse range of future threats (*39*). A detailed understanding of immuno-epidemiological dynamics will be critical to predicting the persistence and community structure of novel pathogens in the future.

REFERENCES AND NOTES

1. P. Rohani, D. J. Earn, B. Finkenstädt, B. T. Grenfell, *Proc. Biol. Sci.* **265**, 2033–2041 (1998).
2. J. O. Lloyd-Smith, *Philos. Trans. R. Soc. B.* **368**, 20120150 (2013).
3. E. W. Seabloom *et al*., *Ecol. Lett.* **18**, 401–415 (2015).
4. A. J. Sieben, J. R. Mihaljevic, L. G. Shoemaker, *Ecology* **103**, e3819 (2022).
5. N. M. Ferguson, A. P. Galvani, R. M. Bush, *Nature* **422**, 428–433 (2003).
6. O. Restif, B. T. Grenfell, *Proc. Biol. Sci.* **273**, 409–416 (2006).
7. B. Adams, A. Sasaki, *Math. Biosci.* **210**, 680–699 (2007).
8. S. Cobey, M. Lipsitch, *Science* **335**, 1376–1380 (2012).
9. N. G. Reich *et al*., *J. R. Soc. Interface* **10**, 20130414 (2013).
10. S. Bhattacharyya, P. H. Gesteland, K. Korgenski, O. N. Bjørnstad, F. R. Adler, *Proc. Natl. Acad. Sci. U.S.A.* **112**, 13396–13400 (2015).
11. S. M. Kissler, C. Tedijanto, E. Goldstein, Y. H. Grad, M. Lipsitch, *Science* **368**, 860–868 (2020).
12. M. Meijers, D. Ruchnewitz, J. Eberhardt, M. Łuksza, M. Lässig, *Cell* **186**, 5151–5164.e13 (2023).
13. N. Ferguson, R. Anderson, S. Gupta, *Proc. Natl. Acad. Sci. U.S.A.* **96**, 790–794 (1999).
14. D. J. Smith *et al*., *Science* **305**, 371–376 (2004).
15. L. J. White, M. Waris, P. A. Cane, D. J. Nokes, G. F. Medley, *Epidemiol. Infect.* **133**, 279–289 (2005).
16. K. Koelle, M. Pascual, M. Yunus, *Proc. Biol. Sci.* **273**, 2879–2886 (2006).
17. T. Bedford, A. Rambaut, M. Pascual, *BMC Biol.* **10**, 38 (2012).
18. R. Grant, L. L. Nguyen, R. Breban, *Bull. World Health Organ.* **98**, 638–640 (2020).
19. W. Yang, E. H. Y. Lau, B. J. Cowling, *PLOS Comput. Biol.* **16**, e1007989 (2020).
20. L. Yan, R. A. Neher, B. I. Shraiman, *eLife* **8**, e44205 (2019).
21. P. Chesson, *Annu. Rev. Ecol. Syst.* **31**, 343–366 (2000).
22. M. Turelli, *Proc. Natl. Acad. Sci. U.S.A.* **75**, 5085–5089 (1978).
23. S. A. H. Geritz, E. Kisdi, G. Meszena, J. A. J. Metz, *Evol. Ecol.* **12**, 35–57 (1998).
24. R. Poulin, S. Morand, *Q. Rev. Biol.* **75**, 277–293 (2000).
25. J. R. Gog, B. T. Grenfell, *Proc. Natl. Acad. Sci. U.S.A.* **99**, 17209–17214 (2002).
26. K. Koelle, S. Cobey, B. Grenfell, M. Pascual, *Science* **314**, 1898–1903 (2006).
27. T. Bedford *et al*., *eLife* **3**, e01914 (2014).
28. C. A. B. Pearson *et al*., Bounding the levels of transmissibility and immune evasion of the Omicron variant in South Africa. medRxiv 2021.12.19.21268038 [Preprint] (2021).
29. R. Earnest *et al*., *Cell Rep. Med.* **3**, 100583 (2022).
30. S. J. Schreiber, J. M. Levine, O. Godoy, N. J. B. Kraft, S. P. Hart, *Ecology* **104**, e3838 (2023).
31. E. Volz *et al*., *Nature* **593**, 266–269 (2021).
32. H. C. Kung, K. F. Jen, W. C. Yuan, S. F. Tien, C. M. Chu, *Bull. World Health Organ.* **56**, 913–918 (1978).
33. D. Hannant, J. A. Mumford, D. M. Jessett, *Vet. Rec.* **122**, 125–128 (1988).
34. J. M. Levine, J. Bascompte, P. B. Adler, S. Allesina, *Nature* **546**, 56–64 (2017).
35. A. Kucharski, J. R. Gog, *Proc. R. Soc. B* **279**, 645–652 2012.
36. B. Bolker, B. Grenfell, *Philos. Trans. R. Soc. B.* **348**, 309–320 (1995).
37. V. Andreasen, G. Dwyer, *Am. Nat.* **201**, 639–658 (2023).
38. H. L. Wells *et al*., *Cell Host Microbe* **31**, 874–889 (2023).
39. M. J. Mina *et al*., *eLife* **9**, e58989 (2020).
40. S. W. Park, parksw3/PIT: archive, Version v1.0.0, Zenodo (2024); https://doi.org/10.5281/zenodo.12610514.
41. G.-Y. Kim, I. Rheem, Y. H. Joung, J. K. Kim, *Respir. Res.* **21**, 191 (2020).
42. S. Takahashi *et al*., *PLOS Med.* **13**, e1001958 (2016).
43. L. C. Katzelnick *et al*., *Science* **358**, 929–932 (2017).

ACKNOWLEDGMENTS

We thank J. Dushoff for helpful discussion and comments on early versions of this manuscript. We thank anonymous reviewers for their valuable comments, especially on pointing out the use of harmonic means to calculate niche and fitness differences in the general case. **Funding:** This work was funded by the following: Princeton Catalysis Initiative (to B.T.G. and C.J.E.M.); Princeton Precision Health (to B.T.G. and C.J.E.M.); Princeton High Meadows Environmental Institute (to B.T.G. and C.J.E.M.); Charlotte Elizabeth Procter Fellowship of Princeton University (to S.W.P.); Peter and Carmen Lucia Buck Foundation Awardee of the Life Sciences Research Foundation (to S.W.P.); National Science Foundation 2022213 (to J.M.L.); National Institute of Allergy and Infectious Diseases, National Institutes of Health, Department of Health and Human Services CEIRR contract 75N93021C00015 (to S.C.). **Author contributions:** Conceptualization: S.W.P., C.J.E.M., J.M.L., and B.T.G. Methodology: S.W.P., S.C., C.J.E.M., J.M.L., and B.T.G. Investigation: S.W.P., S.C., C.J.E.M., J.M.L., and B.T.G. Visualization: S.W.P., J.M.L., and B.T.G. Supervision: C.J.E.M., J.M.L., and B.T.G. Writing – original draft: S.W.P., C.J.E.M., J.M.L., and B.T.G. Writing – review and editing: S.W.P., S.C., C.J.E.M., J.M.L., and B.T.G. **Competing interests:** The authors declare no competing interests. **Data and materials availability:** All data used in this paper are publicly available in references provided in Fig. 1. All code used in this paper are available on GitHub Repository (*40*). **License information:** Copyright © 2024 the authors, some rights reserved; exclusive licensee American Association for the Advancement of Science. No claim to original US government works. https://www.science.org/content/page/science-licenses-journal-article-reuse

SUPPLEMENTARY MATERIALS

science.org/doi/10.1126/science.adq0072
Materials and Methods
Supplementary Text
Figs. S1 to S12
References (*44–50*)
MDAR Reproducibility Checklist

Submitted 22 April 2024; accepted 5 September 2024
10.1126/science.adq0072